Robust Power Control for Wind Power Generation system based on PMSG

NADA ZINE LAABIDINE & AFRAE ERRARHOUT, CHAKIB EL BAKKALI, KARIM MOHAMMED, BADRE BOSSOUFI
LIMAS Laboratory, Faculty of Sciences Dhar El Mahraz, Sidi Mohamed Ben Abdellah University, Fez, MOROCCO

Abstract: In this work, we are developing a new control strategy for wind systems based on the permanent magnet synchronous generator (PMSG). The SMC sliding mode technique is based on the principle of Lyapunov stability in order to make a nonlinear system close to linearity. the use of such a technique with an improvement in regulators to suppress the Chattering phenomenon shows a great improvement in the performance of wind systems. The performance and robustness of the PMSG and the wind turbine are analyzed and compared by simulation based on Matlab / Simulink.

Key-Words: Wind power generator system; SMC Control; PMSG; MPPT; MATLAB/SIMULINK)

Received: December 3, 2019. Revised: May 2, 2020. Accepted: May 18, 2020. Published: June 29, 2020.

1. Introduction

In the recent decades, the scarcity of fossil fuels and their impact on the environment have led to increase the usage of alternative energy resources, such as wind and solar energy. Hence, the growing interest about the electrical energy produced from the wind power from the industries.

There are several research studies about the wind turbine. In particular, the ones with asynchronous generators. Although, they have a low cost and easy maintenance as advantage but, they require more expensive equipment and complex control. Therefore, in the recent years, the Wind Energy Conversion System (WECS) moved towards the Permanent Magnet Synchronous Generators (PMSGs) which have higher efficiency and larger power density.

Furthermore, the PMSG reduces the mechanical stress by removing the necessity of the gear box which improves the system's reliability and decreases the maintenance costs by directly coupling the turbine and the shafts of the generator.

Due to the high variability of the wind speed, it's difficult to obtain a satisfactory performance of the Wind Energy Conversion System (WECS). Recently, this latter is designed to extract the maximum power from the wind speed, which is commonly known as the Maximum Power Point Tracking (MPPT). Different methods have been developed in order to maintain the operating point of maximum efficiency. The most widespread control strategy is the Optimum Power/Torque Tracking, where the use of the proportional and integral (PI) controller. However, this strategy alone doesn't realize a better performance. Hence, there are other control methods such as the Backstepping, fuzzy logic, sliding mode control (SMC), etc.

The aim of this paper is to implement the sliding mode control on the Wind Energy Conversion System (WECS) with a Permanent Magnet Synchronous Generator (PMSG) to achieve a better performance.

The sliding Mode Control (SMC) theory was proposed in the early 1950s, for the context of the variable structure systems (VSS). Though, in the last years, it has become so popular and shown to be a very effective control method, since it is insensitive to the uncertainties and the external disturbances of the system, consequently assuring a good robustness, quick response, stability and easy realization and implementation.

This paper is structured as follows: Section 2 describes the Wind Energy Conversion System (WECS) and presents the mathematical model of the (PMSG) and the back-to-back dc-link converter. Section 3 gives the design of the sliding Mode Control (SMC) for the dynamical model of the PMSG in d-q frame. Section 4 presents and discusses the simulation results. Finally, Section 5 concludes the paper.

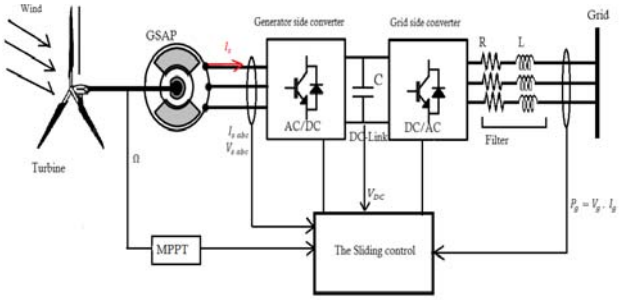

Figure 1. Sliding Mode Control for the WECS

2. Modeling of Wind Turbines

The global wind system is composed of: wind turbine that ensured the kinetic energy converted into mechanical energy than into electrical energy produced by the permanent magnet synchronous generator (PMSG), two converters, one is connected to the Stator and the other to the Grid (Fig.1).

2.1. The model of wind turbine

- The wind power extracted from the wind by the turbine depends on the surface to be swept S, air density and wind speed:

$$P_{wind} = \frac{\rho S V^3}{2} \quad (1)$$

- The power captured by the wind is presented as following:

$$P_{tur} = \frac{\rho \pi R^2 V^3 C_P(\lambda,\beta)}{2} \quad (2)$$

- The power coefficient is defined by the ratio of the power captured by the turbine on the power of the wind and represents the maximum defined by the Betz limit:

$$C_P = \frac{P_{tur}}{P_{wind}} \quad (3)$$

- C_P depends on the pitch angle (β) and the tip speed ratio (λ) :

$$\lambda = \frac{R\omega}{V} \quad (4)$$

- we can deduce the expression of the aerodynamic torque:

$$\begin{cases} P_{tur} = \omega \,.\, T_{tur} \\ T_{tur} = \frac{1}{2}\,[\rho \pi R^3 V^2 C_P(\lambda,\beta)] \end{cases} \quad (5)$$

- In order to insure the maximum efficiency of the wind turbine, the power coefficient (C_P) should be upheld to its maximum.

$$\begin{cases} T_{tur\_opt} = K\omega^2 \\ K = \frac{1}{2}\left[\rho \pi R^5 C_{P-max}(\lambda_{opt})\right] \end{cases} \quad (6)$$

λ_{opt} represents the optimal tip speed ratio that maximizes the power extracted by the wind turbine.

With:

- P_{tur}, the power captured by the wind turbine.
- T_{tur_opt}, the optimal turbine torque.
- T_{tur}, the turbine torque.
- C_p, the power coefficient.
- S, the blade swept area.
- R, the radius of the turbine blade.
- ρ, the specific density of air.
- V, the wind speed.
- ω, the rotor radium.
- λ, tip-speed ratio.
- β, pitch angle.

2.2. The model of PSMG

By using the Park's transform to change the abc coordinate frame model to the d-q coordinate frame model, the permanent magnet synchronous generator equations are presented as following.

- Stator voltages:

$$\begin{cases} V_{sd} = R_S \,.\, I_{sd} + \frac{d\psi_d}{dt} - \omega_r \,.\, \psi_q \\ V_{sq} = R_S \,.\, I_{sq} + \frac{d\psi_q}{dt} + \omega_r \,.\, \psi_d \end{cases} \quad (7)$$

- Stator flux:

$$\begin{cases} \psi_d = L_d \,.\, I_{sd} + \Phi_f \\ \psi_q = L_q \,.\, I_{sq} \end{cases} \quad (8)$$

From (7) and (8) the stator voltages can be written as:

$$\begin{cases} V_{sd} = R_S \,.\, I_{sd} + L_d \frac{dI_{sd}}{dt} - \omega_r \,.\, L_q \,.\, I_{sq} \\ V_{sq} = R_S \,.\, I_{sq} + L_q \frac{dI_{sq}}{dt} + \omega_r \,.\, L_d \,.\, I_{sd} + \omega_r \,.\, \Phi_f \end{cases} \quad (9)$$

The electromagnetic torque is defined, in the d-q synchronously rotating reference frame, as:

$$\begin{cases} T_{tur} - T_{em} = J \,.\, \frac{d\Omega}{dt} + f_C \,.\, \Omega \\ T_{em} = \frac{3}{2} \,.\, p\left[\left(L_d - L_q\right) I_{sd} \,.\, I_{sq} + I_{sq} \,.\, \Phi_f\right] \end{cases} \quad (10)$$

Moreover, the active and reactive powers expressions can be calculated according to the following equations:

$$\begin{cases} P_{gen} = \frac{3}{2}\left[V_{sd} I_{sd} + V_{sq} I_{sq}\right] \\ Q_{gen} = \frac{3}{2}\left[V_{sq} I_{sd} - V_{sd} I_{sq}\right] \end{cases} \quad (11)$$

With

ψ_d, ψ_q, d-q axis flux.

L_d, L_q , d-q axis inductance.

V_{sd}, V_{sq}, d-q axis stator voltage.

I_{sd}, I_{sq} , d-q axis stator current.

T_{em}, Electromagnetic generator torque.

P_{gen}, Active generator power.

Q_{gen}, Reactive generator power.

Ω, Mechanical generator speed.

Φ_f, Generator flux.

f_c, Coefficient of friction.

p the number of poles pairs.

J, the total moment of inertia.

2.3. Model of converters

In order to connect the electrical power to the grid so its converted to DC power then it enter an inverter to convert it to AC power compatible with the grid, this converter called traditional back-to back converter. In order to facilitate modeling and reduce the simulation time, the rectifier is modeled by a set of ideal switches: that is to say zero resistance in the on state, infinite resistance in the off state, instantaneous reaction to control signals.

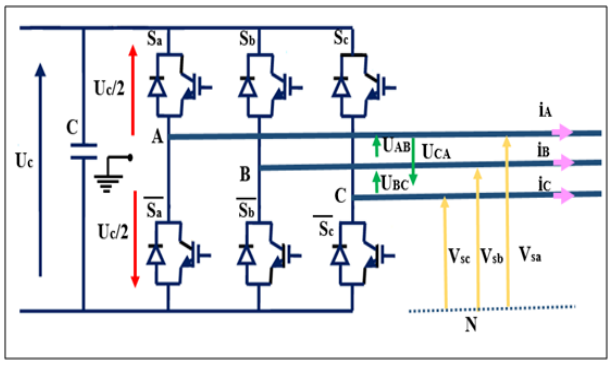

Figure 2. Converter Model

$$S = \begin{cases} +1, \bar{S} = -I \\ -1, \bar{S} = +I \end{cases}, S = a, b, c \quad (12)$$

The input voltages between phases of the converter can be described by:

$$\begin{cases} U_{AB} = V_{AO} - V_{BO} \\ U_{BC} = V_{BO} - V_{CO} \\ U_{CA} = V_{CO} - V_{AO} \end{cases} \quad (13)$$

At the load level, the simple voltages are expressed by:

$$\begin{cases} U_{AB} = V_A - V_B \\ U_{BC} = V_B - V_C \\ U_{CA} = V_C - V_A \end{cases} \quad (14)$$

We can deduce the matrix form of the simple tensions:

$$\begin{bmatrix} V_A \\ V_B \\ V_C \end{bmatrix} = \frac{1}{3} \begin{bmatrix} 2 & -1 & -1 \\ -1 & 2 & -1 \\ -1 & -1 & 2 \end{bmatrix} \begin{bmatrix} V_{AO} \\ V_{BO} \\ V_{CO} \end{bmatrix} \quad (15)$$

With $$\begin{bmatrix} v_{AO} \\ v_{BO} \\ v_{CO} \end{bmatrix} = \frac{U_{CC}}{2} \begin{bmatrix} S_A \\ S_B \\ S_C \end{bmatrix} \quad (16)$$

The simple voltages delivered by the converter will be obtained directly from the states of the control quantities S_A, S_B and S_C which represent the control signals of the switches:

$$\begin{bmatrix} v_A \\ v_B \\ v_C \end{bmatrix} = \frac{U_{CC}}{6} \begin{bmatrix} 2 & -1 & -1 \\ -1 & 2 & -1 \\ -1 & -1 & 2 \end{bmatrix} \begin{bmatrix} S_A \\ S_B \\ S_C \end{bmatrix} \quad (17)$$

2.4. Model of DC bus

The DC bus allows the transfer of power between two different frequency sources; it is used to connect the two converters of the wind system to each other.

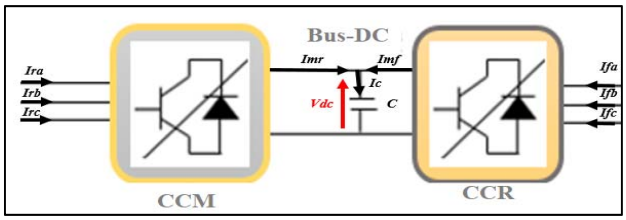

Figure 3. DC-Bus Model

The equations for the DC bus are:

$$\begin{cases} W_{dc} = \int P_c \, . dt = \frac{1}{2} . C . V_{dc}^2 \\ \frac{dV_{dc}^2}{dt} = \frac{2}{C} (P_f - P_r) \end{cases} \quad (18)$$

2.5. Model of RL filter:

The currents passed between the converter and the grid is imposed by the coils constituting the low pass filter.

The three-phase voltages across the filter are:

$$\begin{bmatrix} v_{f1} \\ v_{f2} \\ v_{f3} \end{bmatrix} = R_f . \begin{bmatrix} i_{f1} \\ i_{f2} \\ i_{f3} \end{bmatrix} + L_f \frac{d}{dt} \begin{bmatrix} i_{f1} \\ i_{f2} \\ i_{f3} \end{bmatrix} + \begin{bmatrix} v_{s1} \\ v_{s2} \\ v_{s3} \end{bmatrix} \quad (19)$$

The filter model in the referential (d, q) is given by:

$$\begin{cases} v_{df} = -R_f . I_{df} - L_f . \frac{dI_{df}}{dt} + \omega_s . L_f . I_{qf} \\ v_{qf} = -R_f . I_{qf} - L_f . \frac{dI_{qf}}{dt} - \omega_s . L_f . I_{df} + v_s \end{cases} \quad (20)$$

$$\begin{cases} P_f = V_{df} . I_{df} + V_{Qf} . I_{Qf} \\ Q_f = V_{df} . I_{df} - V_{Qf} . I_{Qf} \end{cases} \quad (21)$$

3. The Sliding Mode Control

The advantages of sliding mode control are significant and multiple, such as high precision, stability, simplicity, a very fast response time low and in particular robustness.

In systems with variable structures with sliding mode, the trajectory state is brought to a surface (hyper plane), then using the switching law, it is obliged to remain in the vicinity of this surface.

The sliding mode control (SMC) is a robust method that has the strength to keep the uncertain systems performance, in various theorical and industrial applications, stable. The SMC controller is designed to systematically take into consideration the stability and the performance problems. This method is divided into three steps:

- Selecting the sliding surface.
- Defining the convergence conditions based on Lyapunov functions.

- Determining the strategy of the control.

3.1. Sliding surface

J.Slotine proposes a form of general equation to determine the sliding surface which ensures the convergence of a variable towards its desired value.

$$S(x,t) = (\frac{d}{dt} + \lambda)^{n-1} . e(t) \quad (22)$$

With,

$e(t)$: the error in the output state $e(t) = x_{ref}(t) - x(t)$.

λ : a positive coefficient.

n : the n^{th}order system. Where for $n = 1$, $S(x,t) = e(t)$.

3.2. The convergence conditions:

The equation of Lyapunov defines the convergence conditions.

$$S(x).\dot{S}(x) < 0 \quad (23)$$

This inequality ensure that the trajectories will remain driven towards their respective sliding surfaces.

3.3. The controller design:

The controller structure entails two parts: a first concerning the exact linearization and a second stabilizing.

$$u(t) = u_{eq}(t) + u_N(t) \quad (24)$$

$u_{eq}(t)$ Corresponds to the equivalent control suggested, It is calculated on basis of the system behavior along the sliding mode described by$\dot{S}(x) = 0$.

$u_N(t)$ is introduced to satisfy the convergence condition $S(x).\dot{S}(x) < 0$, which is defined by the sign of the sliding surface multiplied by a positive constant K.

$$u_N(t) = K\ sgn(S(x)) \quad (25)$$

Where:

$$sgn(S(x)) = \begin{cases} 1 & S(x) > 0 \\ 0 & S(x) = 0 \\ -1 & S(x) < 0 \end{cases} \quad (26)$$

K: is the control gain.

4. The Sliding Mode applied on PSGM

The SMC created based on the mathematical model of the PSGM. For the order system n=1, the manifold equations can be presented as follow:

$$\begin{cases} S(\Omega) = e(\Omega) = \Omega_{ref} - \Omega \\ S(I_{ds}) = e(I_{ds}) = I_{ds_{ref}} - I_{ds} \\ S(I_{qs}) = e(I_{qs}) = I_{qs_{ref}} - I_{qs} \end{cases} \quad (27)$$

4.1. The direct stator current controller

The controller design of the direct current is defined as following:

$$\dot{S}(I_{sd}) = \dot{I}_{sd_{ref}} - \dot{I}_{sd} \quad (28)$$

$$\dot{S}(I_{sd}) = \dot{I}_{sd_{ref}} + \frac{R_S}{L_d} . I_{sd} - p.\Omega . \frac{L_q}{L_d} . I_{sq} - \frac{1}{L_d} V_{sd} \quad (29)$$

The control voltage $V_{sd_{ref}}$is obtained by:

$$V_{sd_{ref}} = V_{sd_{eq}} + V_{sd_N} \quad (30)$$

$$V_{sd_{eq}} = L_d \left[\dot{I}_{sd_{ref}} + \frac{R_S}{L_d} . I_{sd} - p.\Omega . \frac{L_q}{L_d} . I_{sq}\right] \quad (31)$$

$$V_{sd_N} = K_d\ sgn(S(I_{sd})) \quad (32)$$

with $K_d > 0$.

4.2. The Quadrature stator current controller

The controller design of the quadrature current is defined as following:

$$\dot{S}(I_{sq}) = \dot{I}_{sq_{ref}} - \dot{I}_{sq} \quad (33)$$

$$\dot{S}(I_{sq}) = \dot{I}_{sq_{ref}} + \frac{R_S}{L_q} I_{sq} + p\Omega \frac{L_d}{L_q} I_{sd} + \frac{p.\Omega}{L_q} \Phi_f - \frac{1}{L_q} V_{sq} \quad (34)$$

The control voltage $V_{sq_{ref}}$is obtained by:

$$V_{sq_{ref}} = V_{sq_{eq}} + V_{sq_N} \quad (35)$$

$$V_{sq_{eq}} = L_q \left[\dot{I}_{sq_{ref}} + \frac{R_S}{L_q} . I_{sq} + p.\Omega . \frac{L_d}{L_q} . I_{sd} + \frac{p.\Omega}{L_q} . \Phi_f\right] \quad (36)$$

$$V_{sq_N} = K_q\ sgn\left(S(I_{sq})\right) \text{ with } K_q > 0. \quad (37)$$

4.3. Speed regulator

The sliding surface and its derivative for the mechanical speed generator are given by:

$$e(\Omega) = \Omega_{ref} - \Omega \quad (38)$$

$$\dot{S}(\Omega) = \dot{\Omega}_{ref} - \frac{F}{J}\Omega - \frac{3p\phi_f}{2J} I_{qs} + \frac{C_r}{J} \quad (39)$$

The control voltage $I_{sq_{ref}}$is obtained by:

$$I_{qs_{ref}} = I_{qs_{eq}} + I_{qs_N} \quad (40)$$

$$I_{qs_{eq}} = \frac{2J}{3p\phi_f}\left[\dot{\Omega}_{ref} + \frac{F}{J}\Omega + \frac{C_r}{J}\right] \quad (41)$$

$$I_{qs_N} = K_\Omega\ sgn(S(\Omega)) \text{ with } K_\Omega > 0. \quad (42)$$

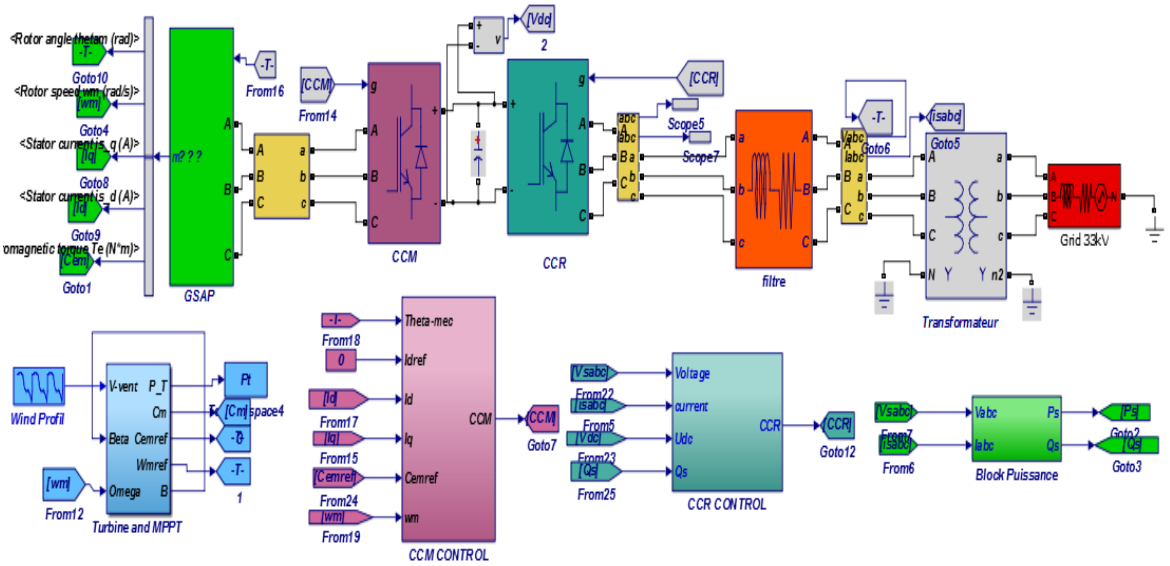

Figure 4. Sliding Mode Control for the WECS in Matlab&Simulink

5. Simulation & Results

The SMC design of the PMSG based WECS was simulated under the MATLAB-Simulink environment. Using the machine's electrical parameters shown in Table1. The sampling frequency chosen is 10 kHz.

The model includes: wind turbine, the permanent magnet synchronous generator, two power converters that connect the stator to the grid and the sliding control. (Fig. 1 & Fig. 2 & Fig.3).

In order to test the robustness of the SMC, we chose a wind profile closer to the evolution of the real wind so that it adapts to the variable wind system to see the degree of continuing point of maximum power (MPPT). We notice that the wind profile and machine angular speed resulted from the simulation follow the same evolution in appropriate manner (Fig. 3 & Fig. 4).

To maximize the electromagnetic torque of the machine with a lesser stator current and to have a better functioning of the complete system, we put the reference direct current isd−ref = 0.

The Fig. 5 and Fig. 6 of the currents verify that the applied SMC provides better performances either at the level of the speed or at the level of the waves provided quality.

The machine is operating in generator mode that's why the active power is negative. We use zero reactive power reference to have a maximum unit power factor and we note that the reactive power progress with that of its zero reference. (Fig.8). From Fig. 6 and Fig. 7 we can see that the active power and the currents produced by the generator have the same profile. Besides, the electrical power tracking with the reference mechanical power is well respected.

In order to validate the SMC, we implement a test with a fluctuating wind profile (Fig.10 & Fig.11). Therefore, the applied SMC offers a good tracking of the setpoints for both the active and reactive power (Fig.14 & Fig.15) and we notice the good quality of the generated currents as shown in Fig.12 & Fig.13.

Therefore, the second test confirms the good follow-up of the previously tracking test.

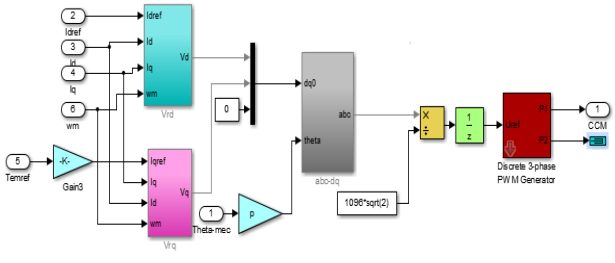

Figure 5. Block diagram of the Sliding Mode control of the Generator Side Converter

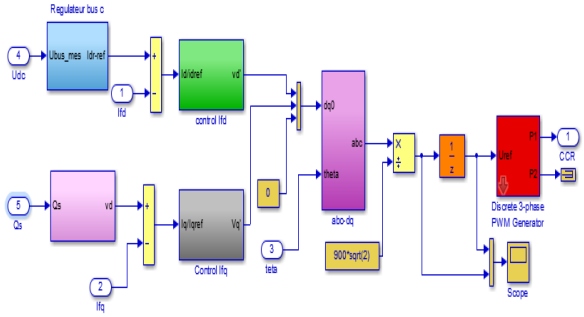

Figure 6. Block diagram of the Sliding Mode control of the Grid Side Converter

5.1. Setpoints tracking test simulation

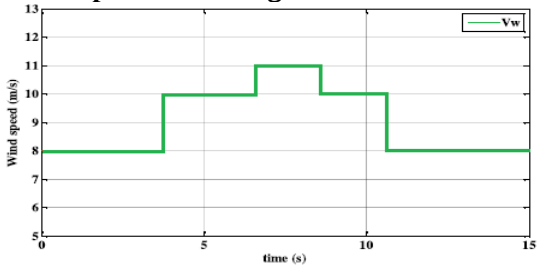

Figure 7.Wind profil

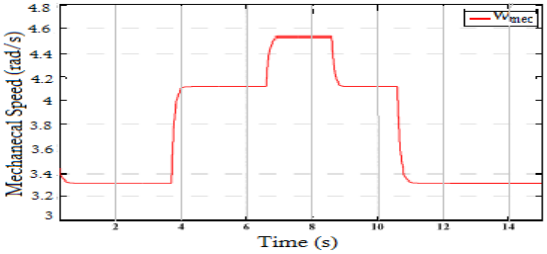

Figure 8. Machanical angular speed

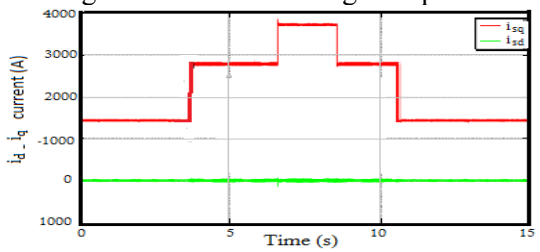

Figure 9. Stator currend i_{sd} _ i_{sq}

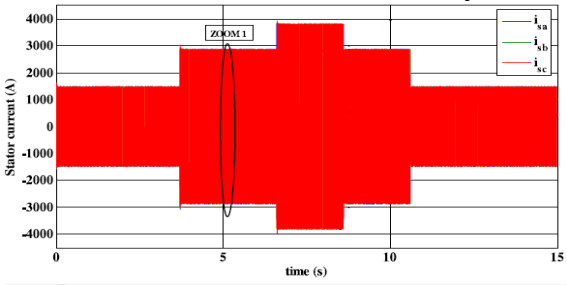

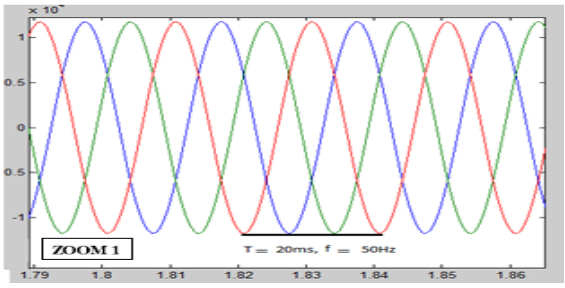

Figure 10. Injected current i_{abc}

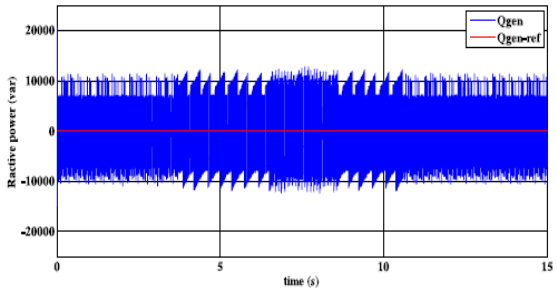

Figure 11. Reactive power generated

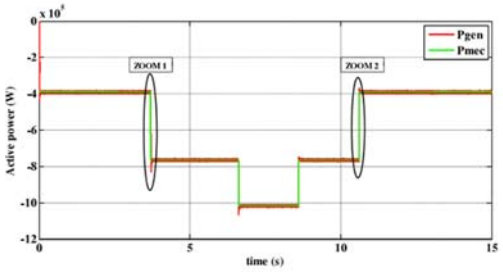

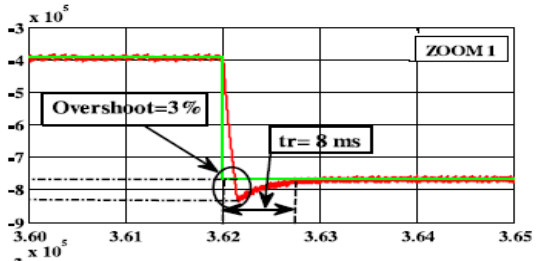

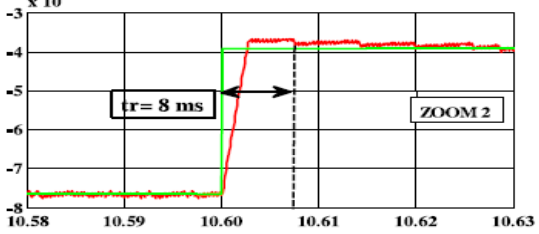

Figure 12. Generator and mechanical power

5.2. Performance for a variable wind speed reference

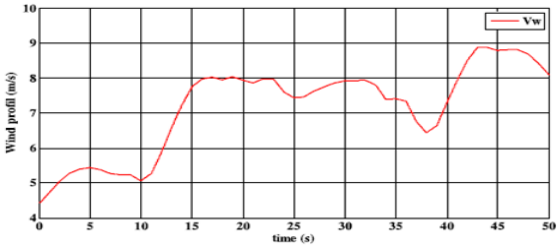

Figure 13. Fluctuating wind speed

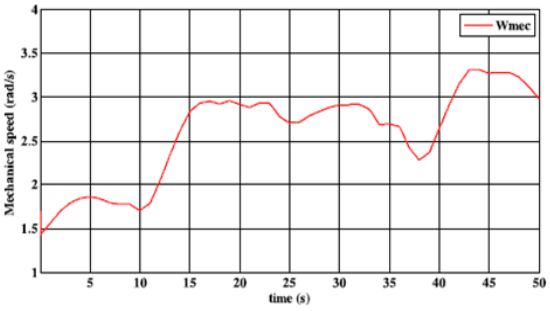

Figure 14. Mechanical angular speed

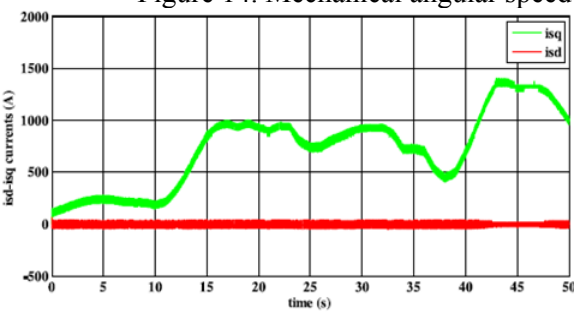

Figure 15. Stator currend i_{sd} _ i_{sq}

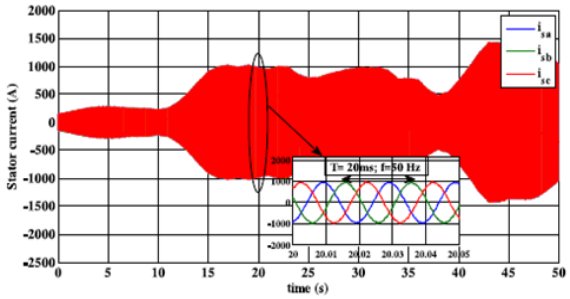

Figure 16. Injected current i_{abc}

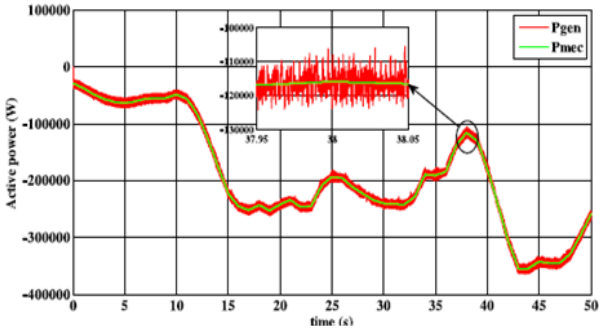

Figure 17. Active power

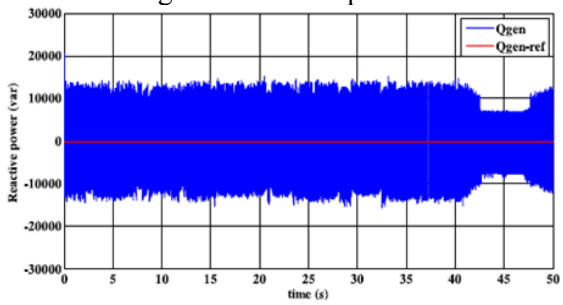

Figure 18. Reactive Power

The first observation lies in the pace of speed that follows the wind profile evolution in an appropriate manner. Power and currents graphs have the same form as the mechanical speed. Tea applied SMC control offers better performances either at the level of speed or at the level of waves provided quality, it is clearly seen through the currents figures illustrated in Fig. 8 and 9. The active power form will have the same profile as that of the currents produced by the generator.

6. Conclusion

A first sliding order of the sliding mode control has been designed and implemented in order to control the output power of a permanent magnet synchronous generator based-WECS. The simulation results prove that the SMC approach is easy to implement and has a quick response with a robust performance against variations in the wind profile and the disturbances in all the system.

References:

[1] X. YU, K. STRUNZ, « Combined long-term and shortterm access storage for sustainable energy system », 2004 IEEE Power Engineering Society General Meeting, vol.2, pp.1946-1951, 10 June 2004.

[2] B.BOSSOUFI, H. ALAMI AROUSSI, EL.M.ZIANI, A.LAGRIOUI, A.DEROUICH "Low-Speed Sensorless Control of DFIG Generators Drive for Wind Turbines System" *WSEAS TRANSACTIONS on SYSTEMS and CONTROL*, pp514-525, Vol.9 No.4 November 2014.

[3] G. Poddar and V. T. Ranganathan, "Direct Torque and Frequency Control of Double- Inverter-Fed Slip-Ring Induction Motor Drive," IEEE Trans. Ind. Electron.,Vol. 51, No. 6, pp. 1329–1337, December 2004.

[4] G. Poddar and V. T. Ranganathan, "Sensorless Double-Inverter-Fed Wound-Rotor Induction-Machine Drive," IEEE Trans. Ind. Electron., Vol. 53, No.1, pp. 86–95, February 2006.

[5] J. Dai, D. Xu, and B.Wu, "A Novel Control Scheme for Current-Source-Converter-Based PMSG Wind Energy Conversion Systems," IEEE Trans. Power Electron., Vol. 24, No. 4, pp. 963–972, April 2009.

[6] H. Akagi and H. Sato, "Control and Performance of a Doubly-Fed Induction Machine Intended for a Flywheel Energy Storage System," IEEE Trans. Power Electron., Vol. 17, No. 1, pp. 109–116, 2002.

[7] Liu, Y., Wang, Z., Xiong, L., Wang, J., Jiang, X., Bai, G., et al., 2018. DFIG wind turbine sliding mode control with exponential reaching law under variable wind speed. Int. J. Electr. Power Energy Syst. 96, 253–260.

[8] Lund, J.W., Boyd, T.L., 2016. Direct utilization of geothermal energy 2015 worldwide review. Geothermics 60, 66–93.

[9] Mahela, O.P., Shaik, A.G., 2016. Comprehensive overview of grid interfaced wind energy generation systems. Renew. Sustain. Energy Rev. 57, 260–281.

[10] Matraji, I., Al-Durra, A., Errouissi, R., 2018. Design and experimental validation of enhanced adaptive second-order SMC for PMSG-based wind energy conversion system. Int. J. Electr. Power Energy Syst. 103, 21–30.

[11] H. ALAMI AROUSSI, El.M. ZIANI, M. BOUDERBALA, B.BOSSOUFI, "Enhancement of the direct power control applied to DFIG-WECS ", International Journal of Electrical and Computer Engineering, Vol. 10, No. 1, pp. 1511~1520, February 2020.

[12] H. Alami Aroussi, El.m. Ziani, M. Bouderbala, B.Bossoufi, "Improvement Of Direct Torque Control Applied To Doubly Fed Induction Motor Under Variable Speed", IJPEDS International Journal of Power Electronics and Drive System. Vol. 11, No. 1, pp. 1511~1520, March 2020.

[13] I. El Karaoui, M.Maaroufi, B.Bossoufi "Comparison of Power Control Methods in Wind Turbines using DFIG: Field Oriented Control and Sliding Mode Control" IJPEDS International Journal of Power

Electronics and Drive System, Vol.11 No.4, December 2019.

[14] F. El Hammouchi, L. El Menzhi, A. Saad, Y. Ihedrane, B.BOSSOUFI "Wind turbine doubly-fed asynchronous machine diagnosis defects using stator and rotor currents lissajous curves" IJPEDS International Journal of Power Electronics and Drive System, Vol.10 No.2, pp 961-971, June 2019.

[15] Y. IHEDRANE, C. EL BEKKALI, M. EL GHAMRASNI, S.MENSOU, B.BOSSOUFI, "Improved Wind System using non-linear Power Control", Indonesian Journal of Electrical Engineering and Computer Science, Vol. 14, No. 3, pp. 1148~1158, June 2019.

[16] Y. IHEDRANE, C. El BEKKALI, B.BOSSOUFI, M. BOUDERBALA "Control of Power of a DFIG Generator with MPPT Technique for Wind Turbines Variable Speed", Renewable Energies book Modeling, Identification and Control Methods in Renewable Energy Systems , SPRINGER, pp 105-129, 25 December 2018.

[17] Y. IHEDRANE, C. El BEKKALI, B.BOSSOUFI "Improved performance of DFIG-Generators for Wind Turbines Variable-Speed" IJPEDS International Journal of Power Electronics and Drive System, Vol.9 No.4, pp1875-1890, December 2018.

[18] M.TAOUSSI, M.KARIM, B.BOSSOUFI, D.HAMMOUMI, A.LAGRIOUI "Low-Speed Sensorless Control for Wind Turbine System" WSEAS TRANSACTIONS on SYSTEMS and CONTROL, pp405-417, Vol.12 No.1, December 2017.

[19] Y. IHEDRANE, C. El BEKKALI, B.BOSSOUFI "Power Control of DFIG-Generators for Wind Turbines Variable-Speed" IJPEDS International Journal of Power Electronics and Drive System, Vol.8 No.1, pp 444-453, March 2017.

[20] B.BOSSOUFI, S.IONITA, H.ALAMI ARROUSSI, M.EL GHAMRASNI, Y.IHEDRANE "Managing voltage drops a variable speed wind turbine connected to the grid" IJAAC International Journal of Automation and Control , Vol.11, No. 1, January 2017.

[21] B.BOSSOUFI, M.KARIM, A.LAGRIOUI, M.TAOUSSI, A.DEROUICH "Observer Backstepping control of DFIG-Generators for Wind Turbines Variable-Speed: FPGA-Based Implementation" Renewable Energy Journal (ELSIVER), pp 903-917, Vol. 81. September 2015.

[22] H.MAHMOUDI, M. EL GHAMRASNI, A. LAGRIOUI, B. BOSSOUFI "Backstepping Adaptive Control Of DFIG-Generators For Wind Turbines Variable-Speed" Journal of Theoretical and Applied Information Technology JATIT, pp 320-330, Vol. 81 No.2, 20th November 2015.

[23] H. ALAMI AROUSSI, El.M. ZIANI, B.BOSSOUFI, "ROBUST CONTROL OF A POWER WIND SYSTEM BASED ON THE DOUBLE FED INDUCTION GENERATOR (DFIG)" Journal of Theoretical and Applied Information Technology JATIT, pp 426-433, Vol. 83 No.3, 31th January 2016.

[24] B.BOSSOUFI, H. ALAMI AROUSSI, El.M.ZIANI, A.LAGRIOUI, A.DEROUICH "Low-Speed Sensorless Control of DFIG Generators Drive for Wind Turbines System" WSEAS TRANSACTIONS on SYSTEMS and CONTROL, pp514-525, Vol.9 No.4 November 2014.

[25] B.BOSSOUFI, M.KARIM, A.LAGRIOUI, M.TAOUSSI, A.DEROUICH "Adaptive Backstepping Control of DFIG Generators for Wide-Range Variable-speed Wind Turbines system" Journal of Journal of Electrical Systems JES, pp317-330. Vol.10 No.3, September 2014.

[26] B.BOSSOUFI, M.KARIM, A.LAGRIOUI, M.TAOUSSI, M.L.EL Hafyani "Backstepping control of DFIG Generators for Wide-Range Variable-Speed Wind Turbines " IJAAC International Journal of Automation and Control , pp 122-140, Vol.8 No.2, July 2014.

[27] B.BOSSOUFI, M.KARIM, A.LAGRIOUI, M.TAOUSSI, M. El GHAMRASNI "Backstepping Adaptive Control of DFIG-Generators for Variable-Speed Wind Turbines" IJCT International Journal of Computers & Technology, pp3719-3733, Vol.12 No.7, February 2014.

[28] B.BOSSOUFI, M.KARIM, A.LAGRIOUI, "FPGA-Based Implementation Sliding Mode Control and nonlinear Adaptive Backstepping control of a Permanent Magnet Synchronous Machine Drive" WSEAS TRANSACTIONS on SYSTEMS and CONTROL, pp86-100, Vol.9 No.1, February 2014.

APPENDIX

TABLE I. THE PMSG AND WIND TURBINE PARAMETERS.

Parameters	Symbol	Values
	Generator	
Power Generator	P_n	1.5 MW
Pole number	p	35
Stator Resistance	R_S	6.25e−3 Ω
d axis inductance	L_d	4.229e−3 H
q axis inductance	L_q	4.229e−3 H
Generator flux	Φ_f	11.1464 Wb
Coefficient of friction	f_c	0 N·m·s/rad
	Wind turbine	
Radius of the turbine blade	R	40 m
Turbine and generator moment	J	1000 N・m
Specific density of air	ρ	1.22 kg/m3
Tip-speed ratio	λ_{opt}	8
Optimal power coefficient	C_{P-max}	0.44